Published in final edited form as:
*Circulation*. 2013 August 13; 128(7): 729–736. doi:10.1161/CIRCULATIONAHA.113.001371.

# Magnetic Resonance $T_1$ Relaxation Time of Venous Thrombus Is Determined by Iron Processing and Predicts Susceptibility to Lysis

**Prakash Saha, MRCS, PhD**[#], **Marcelo E. Andia, MD, PhD**[#], **Bijan Modarai, FRCS, PhD**, **Ulrike Blume, PhD**, **Julia Humphries, PhD**, **Ashish S. Patel, MRCS, PhD**, **Alkystis Phinikaridou, PhD**, **Colin E. Evans, PhD**, **Katherine Mattock, PhD**, **Steven P. Grover, BSc**, **Anwar Ahmad, MRCS**, **Oliver T. Lyons, MRCS**, **Rizwan Q. Attia, MRCS**, **Thomas Renné, MD, PhD**, **Sobath Premaratne, MRCS**, **Andrea J. Wiethoff, PhD**, **René M. Botnar, PhD**, **Tobias Schaeffter, PhD**, **Matthew Waltham, MA, PhD, FRCS**, and **Alberto Smith, PhD**
Academic Department of Surgery, Cardiovascular Division, Kings College London, BHF Centre of Research Excellence & NIHR Biomedical Research Centre at Kings Health Partners, St Thomas' Hospital, London, UK (P.S., B.M., J.H., A.S.P., C.E.E., K.M., S.P.G., A.A., O.T.L., R.Q.A., S.P., M.W., A.S.); Division of Imaging Sciences and Biomedical Engineering, Kings College London, BHF Centre of Research Excellence & Wellcome Trust - EPSRC Medical Engineering Centre & NIHR Biomedical Research Centre at Kings Health Partners, St. Thomas' Hospital, London, UK (M.E.A., U.B., A.P., A.J.W., T.S.); Radiology Department, School of Medicine, Pontificia Universidad Catolica de Chile, Santiago, Chile (M.E.A.); Department of Molecular Medicine and Surgery, Karolinska Institutet and University Hospital Solna, Stockholm, Sweden (T.R.); and Philips Healthcare, Guildford, UK (A.J.W.).

[#] These authors contributed equally to this work.

## Abstract

**Background—**The magnetic resonance longitudinal relaxation time ($T_1$) changes with thrombus age in humans. In this study, we investigate the possible mechanisms that give rise to the $T_1$ signal in venous thrombi and whether changes in $T_1$ relaxation time are informative of the susceptibility to lysis.

**Methods and Results—**Venous thrombosis was induced in the vena cava of BALB/C mice, and temporal changes in $T_1$ relaxation time correlated with thrombus composition. The mean $T_1$ relaxation time of thrombus was shortest at 7days following thrombus induction and returned to that of blood as the thrombus resolved. $T_1$ relaxation time was related to thrombus methemoglobin formation and further processing. Studies in inducible nitric oxide synthase (*iNOS*$^{-/-}$)–deficient mice revealed that inducible nitric oxide synthase mediates oxidation of erythrocyte lysis–derived iron to paramagnetic $Fe^{3+}$, which causes thrombus $T_1$ relaxation time shortening. Studies using chemokine receptor-2–deficient mice (*Ccr2*$^{-/-}$) revealed that the return of the $T_1$ signal to that of blood is regulated by removal of $Fe^{3+}$ by macrophages that accumulate in the thrombus during its resolution. Quantification of $T_1$ relaxation time was a good predictor of successful thrombolysis



Correspondence to Alberto Smith, PhD, Academic Department of Surgery, Cardiovascular Division, King's College London, 1st Floor North Wing, St Thomas' Hospital, Westminster Bridge Rd, London, UK, SE1 7EH. alberto.smith@kcl.ac.uk.
Drs Waltham and Smith are joint senior authors.

**Disclosures:** The MRI scanner is supported in part by Philips Healthcare, Best. Dr Wiethoff is an employee of Philips Healthcare. All other authors were not consultants or employees of Philips Healthcare and had control of inclusion of any data that might present a conflict of interest for Dr Wiethoff. The other authors report no conflicts.


Europe PMC Funders Author Manuscripts

with a cutoff point of <747 ms having a sensitivity and specificity to predict successful lysis of 83% and 94%, respectively.

**Conclusions—**The source of the $T_1$ signal in the thrombus results from the oxidation of iron (released from the lysis of trapped erythrocytes in the thrombus) to its paramagnetic $Fe^{3+}$ form. Quantification of $T_1$ relaxation time appears to be a good predictor of the success of thrombolysis.

### Keywords

macrophages; magnetic resonance imaging; therapeutic thrombolysis; venous thrombosis

Deep venous thrombosis (DVT) affects 1 in 500 of the elderly population per year.[1] Its sequelae include pulmonary embolism, which may be fatal, and the postthrombotic syndrome, which causes chronic morbidity such as leg ulceration that is both debilitating and expensive to treat.[2] The diagnosis of DVT is challenging because the symptoms and signs are nonspecific.[3] Confirmation of thrombosis relies on imaging, but current methods provide little information on thrombus structure or composition, and thrombus burden is generally assessed by the presence or absence of a filling defect in the vein.

The speed of thrombus resolution is the main determinant of subsequent outcome following DVT, both in terms of valve preservation and long-term complications.[4-6] Catheter-directed thrombolysis can reduce postthrombotic syndrome in patients with acute proximal DVT,[7] and, with the increasing use of pharmacomechanical delivery systems that have potential to improve the efficiency of thrombolysis, the paradigm for the management of patients with DVT is changing.[8] Currently, only fresh thrombi are considered for lysis, because it is thought that the collagenous, older thrombi are less responsive to this treatment. The use of clinical history recalled by the patient and signs at presentation are subjective, however, and an unreliable method for estimating thrombus age, and there is no consensus defining the exact timing for intervention.[8] Not all thrombi defined as fresh respond to lysis, exposing the patient to an unnecessary risk of hemorrhage associated with this treatment; whereas some older thrombi have an effective lytic response.[9] An objective method to identify thrombi susceptible to lysis would, therefore, improve the care of patients presenting with thrombosis.

Advances in MRI have made it possible to image venous thrombi with high sensitivity (MR direct thrombus imaging).[10] This method relies on the shorter longitudinal $T_1$ relaxation time of the thrombus in comparison with blood. Spatial quantification of the longitudinal relaxation time is made possible by using a $T_1$-mapping technique that we have previously employed in humans.[11] The biological correlate of the $T_1$ relaxation time is not known, however. In vitro studies suggest that changes in $T_1$ are caused by the accumulation of methemoglobin (metHb) in the thrombus,[12] but this has not been validated in vivo because venous thrombi are not routinely removed from patients. In this study, we use an experimental murine model of venous thrombosis to investigate the mechanisms that give rise to the $T_1$ signal in vivo and examine whether $T_1$ is informative of the susceptibility of thrombus to lysis.

## Methods

### Study Approval

Mouse procedures were performed under the UK Animals (Scientific Procedures) Act, 1986. Ethical approval for the collection of human blood samples was obtained from the local research ethics committee at Guy's & St Thomas' NHS Foundation Trust.

### Generation of metHb In Vitro

Five milliliters of blood was collected from 8- to 10-week-old (22–30 g) male BALB/C mice and human volunteers into 3.2% sodium citrate by using standard venipuncture techniques. Ten milligrams of diethylamine NONOate (Merck) was dissolved into 1.25 mL of 0.9% saline to make a 4 mmol/L solution. Several concentrations (400, 300, 200, 100, and 0 μmol/L) of NONOate were prepared by dilution with normal saline, and 0.1 mL of each solution added to separate aliquots of human and mouse blood. Containers were incubated in a water bath at 37°C for 15 minutes. Samples were imaged by the use of MRI before analysis for metHb with the use of a blood gas analyzer (Roche). metHb measurements for human and murine blood were validated in 20 separate samples by the use of an established colorimetric method.[13]

### Animal Model

Venous thrombosis was induced in the inferior vena cava (IVC) of 8- to 10-week-old (22–30 g) male mice in a surgical procedure that involved a combination of reduced blood flow and endothelial disturbance. The infrarenal portion of the IVC was exposed through a mid-line laparotomy, and a 5-mm segment of the IVC just below the left renal vein was dissected out. A length of 5-0 polypropylene suture was placed alongside the IVC, and a 4–0 silk ligature (Ethicon Ltd) was passed around the IVC, incorporating the polypropylene suture just below the left renal vein. The ligature was tightened and tied, and the polypropylene was withdrawn, leaving a stenosis in the IVC causing an ≈80% to 90% reduction in blood flow. Endothelial damage to this portion of the IVC was then induced by the application of a neurosurgical vascular clip (Braun Medical) for 15 s on 2 occasions, 30 s apart.

### MRI Methods

Mice were imaged with the use of a clinical 3-Tesla Achieva Gyroscan MR scanner (Philips Healthcare, Best, The Netherlands) with a clinical gradient system (30 mT/m, 200 mT/m per ms). The rationale for use of a clinical scanner instead of a preclinical high-field system was to facilitate the translation of the results into clinical practice. All the images were acquired by using a dedicated 47-mm, single-loop, small-animal surface receiver coil to maximize the MR signal. Mice were anesthetized with 1.5% to 2% isoflurane and 100% oxygen delivered through a nose cone and scanned in prone position. Mice were monitored with the use of an MRI-compatible video camera system (Philips Healthcare, Best, The Netherlands). To quickly identify mouse anatomy, an initial survey scan was acquired. Scout imaging was performed by using low-resolution, multiplanar images with a multislice, segmented, fast gradient echo pulse sequence. The field of view of the scout images encompassed the full dimensions of the mouse body. A flow-sensitive time-of-flight sequence was used to identify the IVC and the abdominal aorta, which was used as a fixed anatomic landmark. The filling defect attributable to the presence of thrombus in the IVC was used as a measure of thrombus volume. The imaging parameters of this spoiled gradient echo sequence were as follows: echo time/repetition time=6.2/40 ms, flip angle=60°, a field of view=20×33mm, slices=80, slice thickness=0.3 mm, acquired matrix=68×110, acquired resolution=0.3×0.3×0.5 $mm^3$ and reconstructed resolution=0.13×0.13×0.5 $mm,^3$ averages=2. The average velocity of blood was measured across the IVC to confirm the presence of a thrombus and to measure the changes in recanalization over time. A phase-contrast sequence was used to quantify blood flow with the following imaging parameters: spatial resolution=100×100 μm, slice thickness=2 mm, repetition time/echo time= 17.5/7.2 ms, flip angle=30°, averages=6, and velocity encoding=15 cm/s.

After the acquisition of the venous and arterial time of flight, the data sets were used to plan the location of a 3-dimensional $T_1$- mapping sequence on the thrombus. The fast $T_1$-mapping sequence consisted of a modified Look-Locker sequence.[14,15] A 3-dimensional

volume covering the infrarenal IVC was planned to acquire 16 time points for each pixel. A long relaxation delay of 3 s after each acquisition was used to ensure magnetization recovery. The other sequence parameters were repetition time/echo time 9.0/4.6 ms and flip angle 10°, field of view=36×22mm, acquired matrix=180×102, measured slice thickness=0.5 mm, acquired resolution=0.2×0.2 mm, reconstructed resolution=0.1×0.1 mm, slices=30, averages=1. Total scan time for this sequence was 28 minutes. $T_1$ maps were calculated for each slice by the use of custom-made software implemented in Matlab (Mathworks, Natick, MA).

## Imaging Schedules

The $T_1$ relaxation time in the region of the IVC without thrombus was measured in 6 mice to provide a baseline value for blood. Initial longitudinal imaging experiments were performed to determine the temporal changes in thrombus $T_1$ relaxation time during resolution. Natural thrombus resolution in our mouse model of thrombosis occurs over a period of 28 days,[16,17] with the majority of the cellular changes occurring between days 1 and 14.[18] We therefore chose to consecutively image at 1, 4, 7, 10, 14, 21, and 28 days after induction. This sequential imaging was performed by using 6 mice, because we have previously found that this number is sufficient to show changes in other MRI parameters in venous thrombi.[19] At 28 days, all thrombi were processed for histological analysis (Figure IA in the online-only Data Supplement).

Further experiments were then performed to examine the relationship between $T_1$ relaxation time, thrombus structure, and thrombus iron content. In a cross-sectional study design, $T_1$ relaxation times of thrombi were measured at 1, 4, 7, 10, 14, and 21 days after induction (n=14 per time point). At each time point, thrombi from 8 mice were harvested and used to measure the total iron (4 mice) and $Fe^{3+}$ concentration (4 mice), whereas thrombi from the remaining 6 mice were processed for histological analysis of fibrin and collagen content (Figure IB in the online-only Data Supplement).

Thrombi were also induced in the IVC of *iNOS*$^{-/-}$ and *Ccr2*$^{-/-}$ mice (n=6 per group) to investigate the iron-processing mechanisms that give rise to the $T_1$ paramagnetic signal. In these strains, thrombus was consecutively imaged at 1, 4, 7, 10, 14, and 21days after induction. A schematic of the imaging protocols is shown in Figure IA in the online-only Data Supplement.

## Histology

The position of the thrombus in relation to anatomic landmarks that were imaged (renal and iliac vessels) was measured before harvest by using a Vernier caliper. All samples were taken en bloc to include the portion of IVC containing thrombus and the aorta from the top of the suture to the confluence of the iliac veins. IVC containing thrombus and aorta were pinned on to cork mats to the same length as that measured before harvest and placed in 10% formalin for 24 hours before being embedded in wax. Thrombus was remeasured before embedding to determine whether any shrinkage had taken place. Paraffin sections (5 μm) were taken at 500-μm intervals throughout the length of the IVC to correspond with MR slices. Sections were stained by using hematoxylin and eosin for anatomic detail and Martius Scarlet Blue for red blood cell, fibrin, and collagen content. Digital images of stained sections were captured and processed by using image analysis software (Image Pro-plus 7, MediaCybernetics) with the percentage area of thrombus containing each stain calculated (Figure II in the online-only Data Supplement). Thrombus fibrin and Martius Scarlet Blue content was validated by the use of immunohistochemistry and Western blotting[20] (Figure III in the online-only Data Supplement).

### Image Analysis

Data sets were exported from the MRI scanner and anonymized. $T_1$ maps were then calculated and imported into OSIRIX for analysis by measuring the value of signal intensities and standard deviations on $T_1$ maps in user-specified regions of interest placed over thrombus by using a threshold of 1300 ms. Independent observers (n=5) were orientated to MRI murine anatomy before analyzing thrombus $T_1$ relaxation time to show the interobserver variability (Figure IV in the online-only Data Supplement).

### Iron Quantification

Inductively coupled mass spectroscopy (PE 200 LC system linked to PerkinElmer Sciex Elan 6100 DRC, PerkinElmer, Boston, MA) was performed on a subset of thrombus samples for total iron concentration quantification. Thrombus was digested in 70% nitric acid at 37°C overnight followed by dilution with deionized water for inductively coupled mass spectroscopy analysis.

A commercially available method was modified to quantify $Fe^{3+}$ content in the thrombus (Quantichrom Iron Assay Kit, BioAssay Systems, CA). This method uses a chromogen that specifically forms a blue-colored complex with $Fe.^{2+}$ Reagents in this kit also reduce any $Fe^{3+}$ within the sample to $Fe^{2+}$, allowing the assessment of total iron concentration. It was possible to calculate the amount of $Fe^{3+}$ within processed thrombi by subtracting $Fe^{2+}$ content of the thrombus from the total iron content. Thrombi from 7 mice per time point were analyzed, 4 of which underwent MRI scans.

### Thrombolysis

IVC thrombi were induced in 36 mice. Mice were imaged between day 2 and day 21 following thrombus induction by the use of the $T_1$-mapping protocol described. Immediately following MRI scanning, 200 μL of tissue plasminogen activator solution (10 mg/kg, Actilyse) was administered via a tail-vein injection over 5 minutes. Phase-contrast images were used to estimate blood flow in the IVC before and 24 hours after thrombolytic therapy. Thrombolysis was considered successful if there was at least an increase of 50% in IVC blood flow in comparison with prelysis blood flow. The imaging protocol is shown in Figure IC in the online-only Data Supplement.

### Statistical Analysis

Data were inserted into PRISM version 5 (GraphPad) for analysis. Continuous data are expressed as mean±standard error of the mean. One-way analysis of variance (ANOVA) was used to measure changes in $T_1$ relaxation time, thrombus size and composition, IVC flow, and thrombus iron content over time, and to determine the relationship between $T_1$ relaxation time and susceptibility to lysis. Two-way ANOVA was used to analyze the difference between red blood cell and iron content over time, changes in $T_1$ relaxation times in individual mice over time, and all comparisons between *iNOS*$^{-/-}$ and *Ccr2*$^{-/-}$ mice and their respective wild-type controls. Post hoc test with appropriate Bonferroni correction was made, and the values after the correction were given.

## Results

### Imaging Murine Venous Thrombi by the Use of MRI

Murine metHb was comparable to human metHb in shortening $T_1$ relaxation time in vitro with $T_1$ shortening dependent on concentration of metHb in both species (Figure V in the online-only Data Supplement, murine blood, $R^2$=0.69, $P$<0.0001, n=25; and human blood, $R^2$=0.74, $P$<0.0001, n=25). An experimental model of venous thrombosis was therefore used

in subsequent experiments. Thrombi in our model of thrombosis naturally resolved over a 4-week period, with thrombus volumes ($mm^3$) decreasing gradually over this time (day 1, 17.6±0.9; day 4, 12.6±0.8; day 7, 10.6±0; day 10, 7.6±0.6; day 14, 4.1±0.4; day 21, 0.9±0.2; day 28, 0.3±0.1, 1-way ANOVA, $P<0.0001$; Figure VI in the online-only Data Supplement).

Phase-contrast flow measurements across the IVC confirmed the presence of thrombus. The average blood flow in the IVC, midway between the confluence of the iliac veins and the renal vessels, was 0.428±0.04 mL/min in the steady state. After almost complete occlusion at day 1, an increase in blood flow (mL/min) was detected in the IVC following thrombosis, and this increased progressively as the thrombus resolved (day 1, 0.007±0.002; day 4, 0.031±0.008; day 7, 0.072±0.015; day 10, 0.193±0.013; day 14, 0.246±0.017; day 21, 0.423±0.019; day 28, 0.448±0.041, 1-way ANOVA, $P<0.0001$; Figure VI in the online-only Data Supplement). There was a significant reduction in flow at days 1, 4, 7, 10, and 14 in comparison with IVC without thrombus (Bonferroni multiple comparison test, $P<0.001$). There was no difference in flow at days 21 and 28 in comparison with flow across the IVC without thrombus (Bonferroni multiple comparison test, $P>0.05$).

### $T_1$ Relaxation Time of the Thrombus

The mean $T_1$ relaxation time of venous blood in mice without thrombus was 1557±25 ms. Thrombus was defined as a volume of tissue within the infrarenal IVC (in which there was a filling defect and reduction in blood flow) with a $T_1$ relaxation time of <1300 ms. This arbitrary cutoff was used, because it was >2 standard deviations from the mean $T_1$ relaxation time of blood. Mean $T_1$ relaxation times (ms) of the thrombus changed following thrombus induction (day 1, 866±19; day 4, 758±12; day 7, 631±18; day 10, 671±21; day 14, 741±23; day 21, 970±29; day 28, 1196±42, $P<0.0001$, 1-way ANOVA; Figure 1 and Figure VII in the online-only Data Supplement). As the thrombus resolved, the $T_1$ relaxation time returned to that of blood. The relationship was similar between individual mice over time (Figure VII in the online-only Data Supplement).

### Red Blood Cells and Iron Content of the Thrombus During Its Resolution

The total thrombus iron content (μg), measured by mass spectrometry, was highest 1 day after induction (day 1, 10.2±2.3; day 4, 6.3±0.6; day 7, 6.2±1.0; day 10, 5.1±0.3; day 14, 4.0±0.1; day 21, 0.5±0.1; Figure 2A), when the red blood cell content was greatest. As the thrombus resolved, iron could still be detected in the thrombus microenvironment despite an absence of red blood cell staining (Figure 2A). The concentration of $Fe^{3+}$ in the thrombus (μg/dL per mg of thrombus) changed with time, and was highest at day 7, when T1 relaxation times were shortest (day 1, 3.1±0.3; day 4, 4.6±0.5; day 7, 6.6±0.8; day 10, 4.6±0.8; day 14, 2.1±0.9; day 21, 0.2±0.1, 1-way ANOVA, $P<0.0001$; Figure 2B).

### Thrombus $T_1$ Relaxation Times in *iNOS*$^{-/-}$ Mice

Thrombus in *iNOS*$^{-/-}$ mice had longer $T_1$ relaxation times (ms) (day 1, 1094±16; day 4, 1048±21; day 7, 962±25; day 10, 882±49; day 14, 950±56; day 21, 1108±50) than *iNOS*$^{+/+}$ controls (day 1, 902±31; day 4, 720±13; day 7, 693±25; day 10, 688±29; day 14, 770±35; and day 21, 1127±40, 2-way ANOVA, $P<0.0001$; Figure 2C and Figure VIII in the online-only Data Supplement), but with no difference in thrombus volume between the 2 groups.

### Thrombus $T_1$ Relaxation Times in Ccr2$^{-/-}$ Mice

$T_1$ relaxation times (ms) of thrombus in *Ccr2*$^{+/+}$ mice shortened and then increased during resolution (day 1, 871±25; day 4, 730±10; day 7, 645±16; day 10, 730±25; day 14, 821±39; day 21, 1222±36), whereas thrombus T1 time in *Ccr2*$^{-/-}$ mice (day 1, 888±31; day 4, 813±42; day 7, 741±51; day 10, 691±29; day 14, 623±49; day 21, 642±53) remained

persistently shorter as resolution progressed (2-way ANOVA, $P<0.0001$; Figure 2D and Figure IX in the online-only Data Supplement). Thrombus resolution was impaired in *Ccr2*$^{-/-}$ mice in comparison with wild-type controls (Figure IX in the online-only Data Supplement).

### Structure of Experimental Venous Thrombi During Resolution

The composition of the thrombus varied spatially and temporally during its resolution (Figure 1B and Figure X in the online-only Data Supplement). Red blood cell content progressively decreased after day 1, with the percentage of thrombus area stained for red blood cells as follows: day 1, 93±1%; day 4, 71±2%; day 7, 28±1%; day 10, 8±1%; day 14, 2±0.2%; day 21, 1±0.2%, day 28, 0.2±0.2% (1-way ANOVA, $P<0.0001$; Figure XB in the online-only Data Supplement). The percentage of thrombus area stained for fibrin increased between days 1 and 10 (day 1, 6±1%; day 4, 38±3%; day 7, 67±1%; day 10, 70±2%; day 14, 54±3%; day 21, 5±1%; day 28, 2±0.5%, 1-way ANOVA, $P<0.0001$; Figure XC in the online-only Data Supplement), after which the collagen content (the percentage of thrombus area stained for collagen) appeared to predominate (day 1, 0±0%; day 4, 0.1±0.03%; day 7, 2±0.2%; day 10, 10±1%; day 14, 23±1%; day 21, 47±2%; day 28, 51±2%, 1-way ANOVA, $P<0.0001$, Figure XC in the online-only Data Supplement). Fibrin staining was greatest in thrombi with the shortest $T_1$ relaxation times, irrespective of thrombus age (Figure 3A).

### Thrombolysis of Experimental Venous Thrombi

Fibrinolysis had the greatest effect in thrombi with the shortest $T_1$ relaxation time, regardless of thrombus age (Figure 3B). Receiver operator curve analysis demonstrated that $T_1$ relaxation time was a good predictor of successful thrombolysis (area under the curve, 0.954, $P<0.0001$; 95% confidence interval, 0.894-1.00). A cutoff point of $T_1$ relaxation time <747 ms had a sensitivity and specificity to predict successful lysis of 83% and 94%, respectively.

## Discussion

In vitro studies suggest that shortening of $T_1$ relaxation time of venous thrombi in humans is caused by the paramagnetic properties of $Fe^{3+}$ in the metHb that accumulates.[12] This, however, has not been validated in vivo. The shortening of $T_1$ relaxation time by murine metHb is comparable to that of human metHb ex vivo, and we therefore optimized a $T_1$-mapping protocol, previously used to image DVT in humans,[11] to analyze thrombus in an established murine model of venous thrombosis.[16,17]

The mean $T_1$ relaxation time of thrombus was shortest at 7 days following thrombus induction and returned to that of blood as the thrombus resolved. The total thrombus iron content, measured by mass spectrometry, was highest 1 day after induction when the red blood cell content was greatest. These heme-containing cells, which are the source of iron in the thrombus, are trapped by the cross-linked fibrin that is generated during thrombogenesis. We speculate that red blood cell lysis, previously described at sites of vascular injury,[21] releases iron into the thrombus microenvironment, and this could explain why relatively higher levels of iron are found despite decreasing red blood cell content.

Paramagnetic $Fe^{3+}$ concentrations increased in the thrombus until day 7, when $T_1$ relaxation time was shortest. Nitric oxide is a powerful inducer of metHb in vitro, whereas inflammatory cell accumulation is a characteristic of thrombus resolution.[18,22] This led us to hypothesize that inducible nitric oxide synthase (iNOS) could be a source of nitric oxide that gave rise to the iron oxidation and $T_1$ shortening observed in this study. Thrombus $T_1$ relaxation times were consistently longer in *iNOS*$^{-/-}$ mice than in wild-type controls,

confirming that nitric oxide production is important for the generation of a $T_1$ signal following induction of venous thrombosis. Other oxidative mechanisms are, however, also likely to be important, because there was moderate shortening in $T_1$ relaxation times observed from thrombi in these mice.

Inflammatory monocytes, characterized by Ly6C expression in the mouse, use iNOS for antimicrobial defense against disease.[23] Macrophage accumulation is a hallmark of venous thrombus resolution,[18,22] and, although their function in thrombosis remains largely speculative, we hypothesized that these were the source of iNOS responsible for nitric oxide production and the oxidation of iron. The CC chemokine receptor 2 is required for the emigration of inflammatory monocytes from the bone marrow and their recruitment to inflammatory tissues.[24] Previous studies show that thrombus resolution is impaired in *Ccr2*$^{-/-}$ mice, and this is associated with a reduced accumulation of macrophages in the thrombus.[25,26] Shortening of $T_1$ relaxation time in thrombi formed in *Ccr2*$^{-/-}$ mice was, however, similar to that in wild-type controls suggesting that inflammatory monocyte/macrophages were not the source of nitric oxide in the thrombus as we had hypothesized. Neutrophils are also capable of producing iNOS and accumulate during early thrombogenesis.[27-29] We therefore speculate that these cells could be the effectors of the thrombus $T_1$ shortening that we observed between days 1 and 7 after induction.

Although the deletion of CC chemokine receptor 2 had no effect on thrombus $T_1$ shortening, an absence of thrombus macrophages in *Ccr2*$^{-/-}$ mice affected $T_1$ relaxation time during the latter phase of thrombus resolution. Hemosiderin-laden macrophages (containing $Fe^{3+}$) are known to accumulate in venous thrombi from both wild-type mice and in humans. Iron in these cells is unable to exert a $T_1$ effect because of the large cluster size and the water insolubility of hemosiderin.[30] Without macrophages, $Fe^{3+}$ remains in the thrombus environment in the latter phases of resolution and exerts a $T_1$ relaxation time–shortening effect. Recent evidence suggests that following intraplaque hemorrhage, the accumulation of heme in macrophages leads to an atheroprotective phenotype in which genes central to cholesterol efflux are induced via activating transcription factor-1.[31] It would be interesting to investigate whether macrophage iron uptake in venous thrombi is important to stimulate thrombus resolution by phagocytosis or through the production of angiogenic, proteolytic, and fibrinolytic factors that influence remodeling.[18]

Thrombolytic treatments are designed to lyse fibrin in venous thrombi, with conventional wisdom suggesting that young thrombi, defined by clinical history, are most readily lysed. In this study, thrombus fibrin content was greatest between days 7 and 10 following induction, the point at which thrombus $T_1$ relaxation time was shortest. Administration of tissue plasminogen activator had the greatest effect in experimental thrombi with the shortest $T_1$, regardless of thrombus age. Older thrombi with high collagen content did not respond well to lysis, but unexpectedly very young thrombi had an equally poor response. There is evidence from studies in humans to show that not all young venous thrombi can be lysed,[9] while early preclinical studies of thrombolysis using tissue plasminogen activator show that this agent more readily lyses 7-day-old thrombi in comparison with 1- or 3-dayold thrombi in a rabbit model of this condition.[32] The results from our study are therefore not all together surprising. One explanation for our finding of impaired lysis in 1- or 4-dayold thrombi could be the result of a shielding effect by red blood cells. Recent in vitro studies show that the presence of red blood cells confers resistance to fibrinolysis through the modification of fibrin structure and impairment of plasminogen activation.[33] Whether a similar mechanism exists in vivo requires further investigation.

## Conclusion

These data shed light on the biological mechanisms that affect $T_1$ relaxation during thrombus resolution in vivo. Iron, brought into the thrombus by fibrin-trapped red blood cells, is oxidized through iNOS, resulting in the accumulation of paramagnetic $Fe^{3+}$, which shortens $T_1$. Removal of $Fe^{3+}$ by the action of macrophages returns $T_1$ relaxation time to that of blood. Quantification of $T_1$ relaxation time was informative of the susceptibility of a thrombus to lysis, whereas our use of a clinical 3-T field strength MRI scanner without a contrast agent facilitates immediate translation of this technique to the clinic.

## Supplementary Material

Refer to Web version on PubMed Central for supplementary material.

## Acknowledgments

We thank Prof Beverly Hunt for supplying the method for the generation of methemoglobin in vitro and Prof Frederic Geissmann for supplying the knockout mice used in this study. We also thank Roshini Joseph for her help with the fibrin quantification and Dr Victoria Cornelius for support with statistical analysis.

**Sources of Funding:** This work was supported by the British Heart Foundation Project grant (PG/08/039/24436, to Drs Schaeffter, Waltham, and Smith), Wellcome Trest (WT090252MA, to Dr Saha), and the Chilean Agency for Research in Science and Technology (CONICYT, to Dr Andia).

## References

1. Fowkes FJ, Price JF, Fowkes FG. Incidence of diagnosed deep vein thrombosis in the general population: systematic review. Eur J Vasc Endovasc Surg. 2003; 25:1–5. [PubMed: 12525804]
2. Kahn SR, Shbaklo H, Lamping DL, Holcroft CA, Shrier I, Miron MJ, Roussin A, Desmarais S, Joyal F, Kassis J, Solymoss S, Desjardins L, Johri M, Ginsberg JS. Determinants of health-related quality of life during the 2 years following deep vein thrombosis. J Thromb Haemost. 2008; 6:1105–1112. [PubMed: 18466316]
3. Mannucci PM, Poller L. Venous thrombosis and anticoagulant therapy. Br J Haematol. 2001; 114:258–270. [PubMed: 11529843]
4. Meissner MH, Caps MT, Zierler BK, Polissar N, Bergelin RO, Manzo RA, Strandness DE Jr. Determinants of chronic venous disease after acute deep venous thrombosis. J Vasc Surg. 1998; 28:826–833. [PubMed: 9808849]
5. Meissner MH, Manzo RA, Bergelin RO, Markel A, Strandness DE Jr. Deep venous insufficiency: the relationship between lysis and subsequent reflux. J Vasc Surg. 1993; 18:596–605. Discussion p. 606. [PubMed: 8411467]
6. Saarinen J, Kallio T, Lehto M, Hiltunen S, Sisto T. The occurrence of the post-thrombotic changes after an acute deep venous thrombosis. A prospective two-year follow-up study. Journal of Cardiovascular Surgery. 2000; 41:441–446. [PubMed: 10952338]
7. Enden T, Haig Y, Kløw NE, Slagsvold CE, Sandvik L, Ghanima W, Hafsahl G, Holme PA, Holmen LO, Njaastad AM, Sandbæk G, Sandset PM. CaVenT Study Group. Long-term outcome after additional catheter-directed thrombolysis versus standard treatment for acute iliofemoral deep vein thrombosis (the CaVenT study): a randomised controlled trial. Lancet. 2012; 379:31–38. [PubMed: 22172244]
8. Patterson BO, Hinchliffe R, Loftus IM, Thompson MM, Holt PJ. Indications for catheter-directed thrombolysis in the management of acute proximal deep venous thrombosis. Arterioscler Thromb Vasc Biol. 2010; 30:669–674. [PubMed: 20237328]
9. Mewissen MW, Seabrook GR, Meissner MH, Cynamon J, Labropoulos N, Haughton SH. Catheter-directed thrombolysis for lower extremity deep venous thrombosis: report of a national multicenter registry. Radiology. 1999; 211:39–49. [PubMed: 10189452]

10. Moody AR. Direct imaging of deep-vein thrombosis with magnetic resonance imaging. Lancet. 1997; 350:1073. [PubMed: 10213551]
11. Blume U, Orbell J, Waltham M, Smith A, Razavi R, Schaeffter T. 3D T(1)-mapping for the characterization of deep vein thrombosis. MAGMA. 2009; 22:375–383. [PubMed: 19946791]
12. Kelly J, Hunt BJ, Moody A. Magnetic resonance direct thrombus imaging: a novel technique for imaging venous thromboemboli. Thromb Haemost. 2003; 89:773–782. [PubMed: 12719772]
13. Leahy T, Smith R. Notes on methemoglobin determination. Clin Chem. 1960; 6:148–152. [PubMed: 14414949]
14. Look DC, Locker DR. Time saving in measurement of NMR and EPR relaxation times. Rev Sci Instrum. 1970; 41:250–251.
15. Messroghli DR, Radjenovic A, Kozerke S, Higgins DM, Sivananthan MU, Ridgway JP. Modified Look-Locker inversion recovery (MOLLI) for high-resolution T1 mapping of the heart. Magn Reson Med. 2004; 52:141–146. [PubMed: 15236377]
16. Singh I, Burnand KG, Collins M, Luttun A, Collen D, Boelhouwer B, Smith A. Failure of thrombus to resolve in urokinase-type plasminogen activator gene-knockout mice: rescue by normal bone marrow-derived cells. Circulation. 2003; 107:869–875. [PubMed: 12591758]
17. Singh I, Smith A, Vanzieleghem B, Collen D, Burnand K, Saint-Remy JM, Jacquemin M. Antithrombotic effects of controlled inhibition of factor VIII with a partially inhibitory human monoclonal antibody in a murine vena cava thrombosis model. Blood. 2002; 99:3235–3240. [PubMed: 11964288]
18. Saha P, Humphries J, Modarai B, Mattock K, Waltham M, Evans CE, Ahmad A, Patel AS, Premaratne S, Lyons OT, Smith A. Leukocytes and the natural history of deep vein thrombosis: current concepts and future directions. Arterioscler Thromb Vasc Biol. 2011; 31:506–512. [PubMed: 21325673]
19. Phinikaridou A, Andia ME, Saha P, Modarai B, Smith A, Botnar RM. ***In vivo*** magnetization transfer and diffusion-weighted magnetic resonance imaging detects thrombus composition in a mouse model of deep vein thrombosis. Circ Cardiovasc Imaging. 2013; 6:433–440. [PubMed: 23564561]
20. Müller F, Mutch NJ, Schenk WA, Smith SA, Esterl L, Spronk HM, Schmidbauer S, Gahl WA, Morrissey JH, Renné T. Platelet polyphosphates are proinflammatory and procoagulant mediators in vivo. Cell. 2009; 139:1143–1156. [PubMed: 20005807]
21. Woollard KJ, Sturgeon S, Chin-Dusting JP, Salem HH, Jackson SP. Erythrocyte hemolysis and hemoglobin oxidation promote ferric chloride-induced vascular injury. J Biol Chem. 2009; 284:13110–13118. [PubMed: 19276082]
22. Wakefield TW, Myers DD, Henke PK. Mechanisms of venous thrombosis and resolution. Arterioscler Thromb Vasc Biol. 2008; 28:387–391. [PubMed: 18296594]
23. Auffray C, Sieweke MH, Geissmann F. Blood monocytes: development, heterogeneity, and relationship with dendritic cells. Annu Rev Immunol. 2009; 27:669–692. [PubMed: 19132917]
24. Serbina NV, Pamer EG. Monocyte emigration from bone marrow during bacterial infection requires signals mediated by chemokine receptor CCR2. Nat Immunol. 2006; 7:311–317. [PubMed: 16462739]
25. Henke PK, Pearce CG, Moaveni DM, Moore AJ, Lynch EM, Longo C, Varma M, Dewyer NA, Deatrick KB, Upchurch GR Jr, Wakefield TW, Hogaboam C, Kunkel SL. Targeted deletion of CCR2 impairs deep vein thombosis resolution in a mouse model. J Immunol. 2006; 177:3388–3397. [PubMed: 16920980]
26. Ali T, Humphries J, Burnand K, Sawyer B, Bursill C, Channon K, Greaves D, Rollins B, Charo IF, Smith A. Monocyte recruitment in venous thrombus resolution. J Vasc Surg. 2006; 43:601–608. [PubMed: 16520180]
27. von Brühl ML, Stark K, Steinhart A, Chandraratne S, Konrad I, Lorenz M, Khandoga A, Tirniceriu A, Coletti R, Köllnberger M, Byrne RA, Laitinen I, Walch A, Brill A, Pfeiler S, Manukyan D, Braun S, Lange P, Riegger J, Ware J, Eckart A, Haidari S, Rudelius M, Schulz C, Echtler K, Brinkmann V, Schwaiger M, Preissner KT, Wagner DD, Mackman N, Engelmann B, Massberg S. Monocytes, neutrophils, and platelets cooperate to initiate and propagate venous thrombosis in mice in vivo. J Exp Med. 2012; 209:819–835. [PubMed: 22451716]

28. Fuchs TA, Brill A, Duerschmied D, Schatzberg D, Monestier M, Myers DD Jr, Wrobleski SK, Wakefield TW, Hartwig JH, Wagner DD. Extracellular DNA traps promote thrombosis. Proc Natl Acad Sci U S A. 2010; 107:15880–15885. [PubMed: 20798043]

29. Darbousset R, Thomas GM, Mezouar S, Frère C, Bonier R, Mackman N, Renné T, Dignat-George F, Dubois C, Panicot-Dubois L. Tissue factor-positive neutrophils bind to injured endothelial wall and initiate thrombus formation. Blood. 2012; 120:2133–2143. [PubMed: 22837532]

30. Vymazal J, Urgosík D, Bulte JW. Differentiation between hemosiderin- and ferritin-bound brain iron using nuclear magnetic resonance and magnetic resonance imaging. Cell Mol Biol (Noisy-le-grand). 2000; 46:835–842. [PubMed: 10875444]

31. Boyle JJ, Johns M, Kampfer T, Nguyen AT, Game L, Schaer DJ, Mason JC, Haskard DO. Activating transcription factor 1 directs Mhem athero-protective macrophages through coordinated iron handling and foam cell protection. Circ Res. 2012; 110:20–33. [PubMed: 22052915]

32. Collen D, Stassen JM, Verstraete M. Thrombolysis with human extrinsic (tissue-type) plasminogen activator in rabbits with experimental jugular vein thrombosis. Effect of molecular form and dose of activator, age of the thrombus, and route of administration. J Clin Invest. 1983; 71:368–376. [PubMed: 6681615]

33. Wohner N, Sótonyi P, Machovich R, Szabó L, Tenekedjiev K, Silva MM, Longstaff C, Kolev K. Lytic resistance of fibrin containing red blood cells. Arterioscler Thromb Vasc Biol. 2011; 31:2306–2313. [PubMed: 21737785]

Europe PMC Funders Author Manuscripts

Europe PMC Funders Author Manuscripts

## CLINICAL PERSPECTIVE

The paradigm of deep venous thrombosis management is changing with a greater focus on restoring vein patency by the use of catheter-directed thrombolysis and pharmacomechanical adjuncts with the aim of reducing the incidence of the post-thrombotic syndrome. Selection criteria used to identify thrombi that are most susceptible to lysis remain controversial. Thrombus age is currently the main determinant for thrombolysis, but clinical history and signs at presentation are subjective and unreliable. Not all young thrombi can be successfully lysed, whereas some old thrombi may be amenable to lysis. In this study, we show that fast $T_1$ mapping can be used as a surrogate measure of the organization of experimental venous thrombi and that this technique identifies those thrombi most suitable for lysis. Experiments in this study were performed with the use of a clinical 3-T field strength MRI scanner without contrast agent, which facilitates the immediate translation of $T_1$ mapping of thrombosis to the clinic.

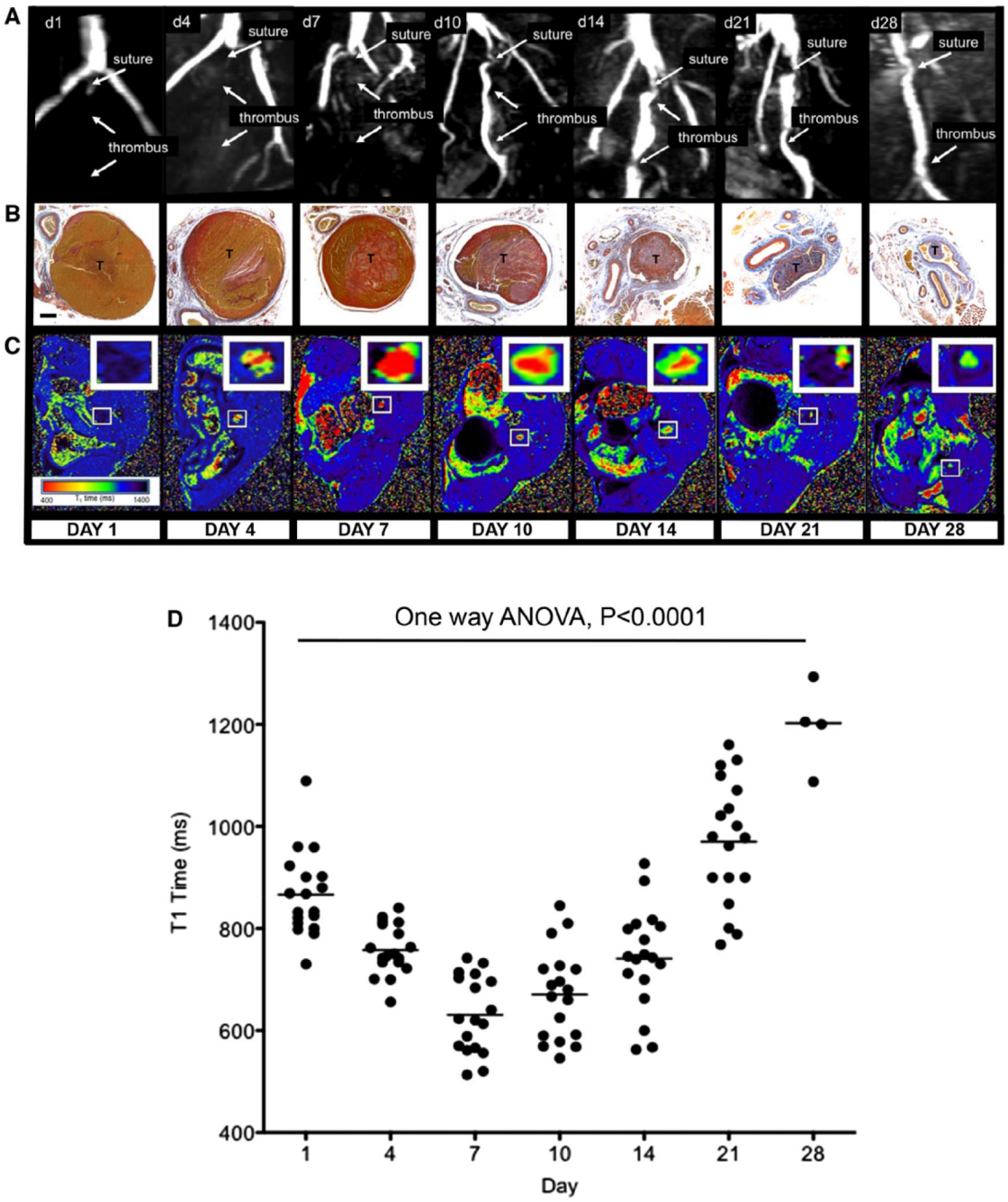


**Figure 1.**

Magnetic resonance $T_1$ mapping of experimental venous thrombi. **A**, MRI venography demonstrates the presence of thrombus in the murine inferior vena cava, which recanalizes over 28 days. **B**, MSB sections of venous thrombus (T) during its resolution (yellow=red cells, red=fibrin, blue=collagen; ×200; bar, 200 μm). **C**, Corresponding $T_1$ maps were generated by the use of a customized program (MATLAB software, MathWorks) before importation into OSIRIX as shown. Short $T_1$ relaxation times (ms) appear red and revert back to blood (black) as thrombus ages. **D**, Mean $T_1$ relaxation times (ms) of the thrombus change during its resolution (scatter plot and mean of thrombus $T_1$ relaxation time [ms] is shown, n=88 mice, $P<0.0001$, 1-way ANOVA). Mouse procedures were performed under

the Animals (Scientific Procedures) Act, 1986, UK. ANOVA indicates analysis of variance; d, day; and MSB, Martius Scarlet Blue.



Europe PMC Funders Author Manuscripts

Europe PMC Funders Author Manuscripts

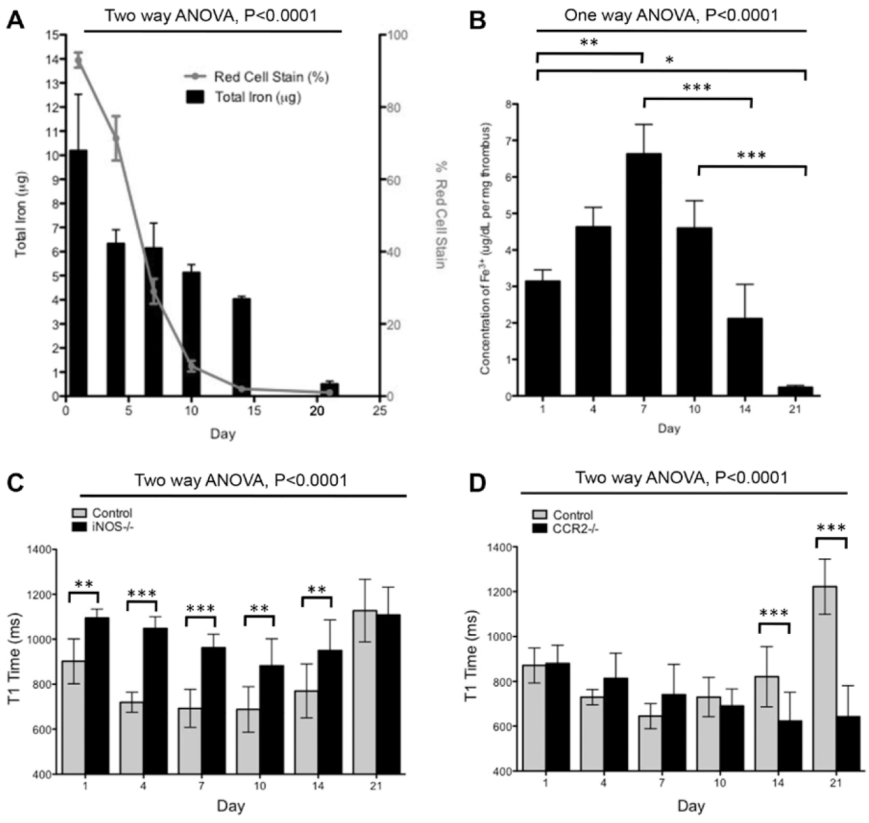


**Figure 2.**

Mechanisms governing the generation of $T_1$ signal in venous thrombi. **A**, The total iron content of the thrombus (black bars) quantified by using mass spectrometry (n=4/gp) is greatest immediately after thrombus induction when red blood cell content (red line) is high (n=6/gp). During thrombus resolution, the iron content falls, but it remains relatively higher than the red blood cell content of the thrombus (mean±SEM shown, $P<0.0001$, 2-way ANOVA). **B**, $Fe^{3+}$ concentration (μg/dL per mg of thrombus) analyzed with the use of a colorimetric iron assay kit at different time points mirrors the $T_1$ signal during thrombus resolution (mean±SEM shown, n=7/gp, $P<0.0001$, 1-way ANOVA with Bonferroni post test analysis. *$P<0.05$, **$P<0.01$, ***$P<0.001$). **C**, $T_1$ relaxation times (ms) of the thrombus are significantly longer during thrombus resolution in *iNOS*$^{-/-}$ in comparison with wild-type controls (mean+SEM, n=6/gp, $P<0.0001$, 2-way ANOVA, Bonferroni post test: **$P<0.01$, ***$P<0.001$). **D**, $T_1$ relaxation times (ms) of the thrombus remain persistently short in *CCR2*$^{-/-}$ mice during resolution (mean+SEM, n=7/gp, $P<0.0001$, 2-way ANOVA, Bonferroni post test: *$P<0.05$, ***$P<0.001$). Mouse procedures were performed under the Animals (Scientific Procedures) Act, 1986, UK. ANOVA indicates analysis of variance; gp, group; and SEM, standard error of the mean.

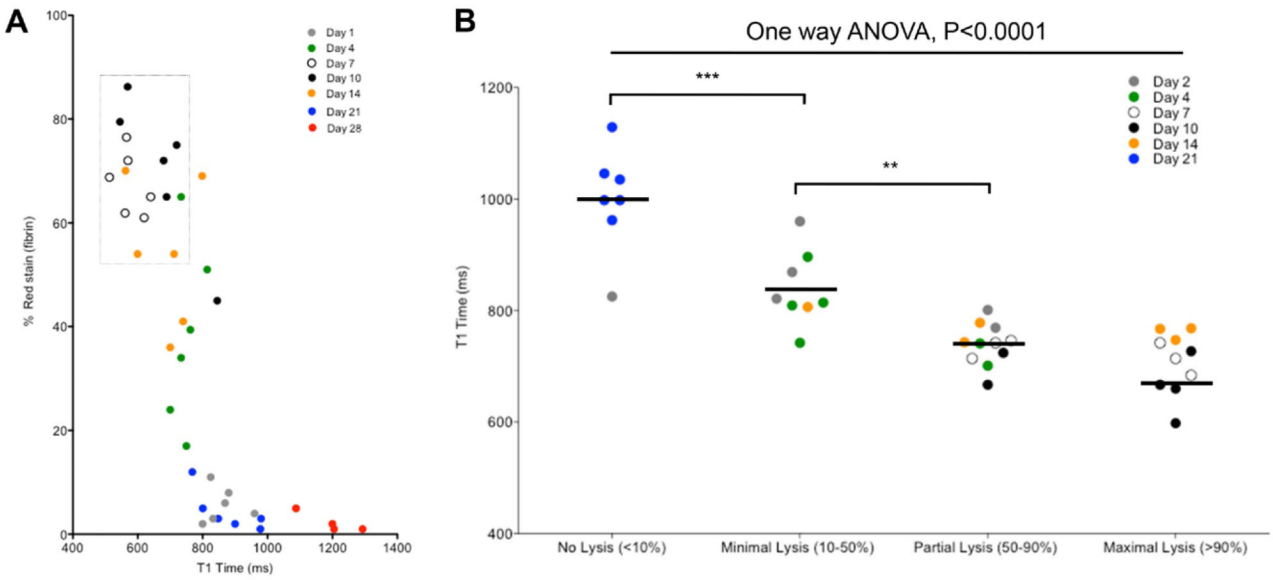


**Figure 3.**

Magnetic resonance $T_1$ mapping can be used to stratify venous thrombi suitable for fibrinolysis. **A**, Percentage of fibrin stain in thrombus during its resolution and $T_1$ relaxation. Short $T_1$ relaxation times are associated with higher amounts of fibrin stain. A strike zone of lysis (dotted box) indicates thrombi that would be suitable for fibrinolytic therapy. **B**, In a separate group of animals, mean $T_1$ maps of thrombi between 2 and 21 days of age were generated (n=36). Blood flow was measured in the inferior vena cava (IVC) before administration of systemic thrombolysis and 24 hours after administration, and groups of mice were divided dependent on their response to lysis. Mouse procedures were performed under the Animals (Scientific Procedures) Act, 1986, UK. ANOVA indicates analysis of variance.




Europe PMC Funders Author Manuscripts